

MORPHOLOGY AND SPECTRAL BEHAVIOR OF SOLAR HARD X-RAY SOURCES

F. C. R. Fernandes and H. S. Sawant

Instituto Nacional de Pesquisas Espaciais (INPE), Brazil

Received 2000 October 23; accepted 2002 May 02

RESUMEN

Las imágenes de 17 fulguraciones solares, correspondiendo a 61 explosiones de rayos-X observados en cuatro rangos de energía (14–23, 23–33, 33–53 y 53–93 keV) por el experimento Hard X-Ray Telescope (HXT) a bordo del satélite *Yohkoh*, han sido investigadas. Las imágenes sugieren que el tamaño de las fuentes de rayos-X duros es del orden de 20 segundos de arco y que existen 3 tipos: fuentes individuales simples ($\sim 30\%$), fuentes dobles ($\sim 41\%$), con separación mínima típica de 30–40 segundos de arco y fuentes múltiples ($\sim 29\%$). Hemos ajustado un único espectro de potencia para las emisiones de rayos-X en el rango de 20–830 keV utilizando datos del experimento Hard X-Ray Spectrometer (HXS). La evolución temporal del espectro de estas explosiones también fue estudiada. El comportamiento típico del índice es “blando-duro-blando”.

ABSTRACT

Images of 17 solar flares, corresponding to 61 individual X-ray bursts observed in four energy bands (14–23, 23–33, 33–53, and 53–93 keV) by the Hard X-Ray Telescope (HXT) experiment aboard the *Yohkoh* satellite have been investigated. The images suggest that the angular size of the hard X-ray sources is of the order of 20 arcsec and that they are of three types: single isolated sources ($\sim 30\%$), double sources ($\sim 41\%$), with typical minimum separation of 30–40 arcsec, and multiple sources ($\sim 29\%$). We have fitted a single power law spectrum to the X-ray emission in the range 20–830 keV, using data from the Hard X-Ray Spectrometer (HXS) experiment. The spectral time evolution of these bursts has been also investigated. Typical spectral index behavior is “soft-hard-soft”.

Key Words: **SUN: FLARES — SUN: X-RAYS**

1. INTRODUCTION

The two main processes by which hard X-ray are produced by the Bremsstrahlung mechanism when non-thermal electron beams interact with an ambient plasma are the thick target and the thin target mechanisms (Brown 1971). Since the electrons carry a significant fraction of the primary energy released during the solar flares, the determination of the spatial, spectral, and temporal evolution of the hard X-ray sources is crucial.

The first bi-dimensional solar images in hard X-rays were taken during the maximum of the 21st solar activity cycle in 1980 by the Hard X-Ray Imaging Spectrometer (HXIS) experiment aboard the *Solar Maximum Mission (SMM)* satellite (Acton et al. 1980), and also by the Solar X-Ray Telescope (SXT) of the *Hinotori* satellite (Kondo 1982). Those im-

agers have moderate spatial resolutions of 8 and 10 arcsec, and they cover energy bands of 3.5–30 keV and 5–40 keV, respectively.

The *SMM* observations of solar flares showed that hard X-rays were emitted from double sources (Hoynig, Machado, & Duijveman 1981; Duijveman, Hoynig, & Machado 1982). The double-source structure was interpreted as corresponding to the footpoints of a coronal magnetic loop, where the electron beams generate hard X-rays by the Bremsstrahlung mechanism. Similar structures were identified from *Hinotori* observations of flares (Takakura et al. 1983).

More precise identification of double hard X-ray sources was obtained from the *Yohkoh* satellite observations (Ogawara et al. 1991). Studies of many events clearly showed that hard X-rays are preferen-

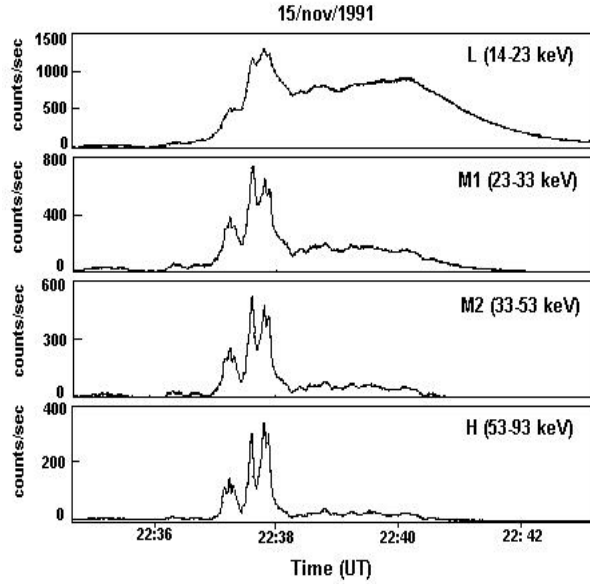


Fig. 1. Time profiles of X-ray bursts (4 energy bands) observed in 1991 November 15 by HXT.

tially emitted by distinct double sources, located at the edges of a single magnetic structure (a loop), on both sides of a magnetic neutral sheet, implying that the double sources are not nearby isolated sources but that they are connected magnetically (Kosugi et al. 1992; Sakao et al. 1996). Also, the X-ray flux in both sources varies simultaneously on time scales < 1 s, suggesting that the emission is due to electron beams traveling through the legs of the same magnetic loop. Analyzing solar flares observed in the limb, Masuda et al. (1995) have found flares in which the hard X-ray sources are located at foot-points of the loops and also above the top of the loop (Masuda 1994).

The analysis of the spectral behavior and its time evolution gives information about the dependence of the X-ray emission on the electron energy distribution, essential for investigations of the acceleration processes of particles during solar flares.

The investigations of the spectral behavior carried out before the *Yohkoh* observations covered energies only up to 580 keV. *Yohkoh* data, covering a wider energy range (up to 830 keV), and with better spectral resolution (32 channels), permit a more precise determination of the spectral index and its temporal evolution.

2. INSTRUMENTATION AND OBSERVATIONS

The Hard X-Ray Telescope (HXT) (Kosugi et al. 1991) aboard the *Yohkoh* satellite is a hard X-ray imaging spectrometer for solar flare observations.

TABLE 1

| HXT BURSTS SELECTED | | | |
|---------------------|-----------|---------------|------------|
| Flare No. | Date | Time (UT) Max | GOES CLASS |
| 1 | 91/Oct/24 | 22:37:50 | M9.8 |
| 2 | 91/Nov/02 | 06:47:00 | M9.1 |
| 3 | 91/Nov/10 | 20:10:02 | M7.9 |
| 4 | 91/Nov/15 | 22:37:50 | X1.5 |
| 5 | 91/Dec/03 | 16:36:41 | X2.2 |
| 6 | 91/Dec/16 | 01:02:02 | C7.5 |
| 7 | 91/Dec/16 | 04:56:10 | M2.7 |
| 8 | 91/Dec/30 | 23:07:10 | M4.6 |
| 9 | 92/Jan/26 | 15:28:39 | X1.0 |
| 10 | 92/Jul/08 | 09:47:57 | X1.2 |
| 11 | 92/Sep/05 | 11:27:02 | M4.0 |
| 12 | 92/Sep/06 | 09:04:08 | M3.3 |
| 13 | 92/Sep/06 | 11:51:26 | M4.0 |
| 14 | 92/Sep/10 | 22:53:05 | M3.2 |
| 15 | 93/Oct/02 | 07:40:10 | C6.5 |
| 16 | 93/Oct/03 | 09:27:32 | C8.6 |
| 17 | 93/Oct/03 | 12:42:42 | C3.0 |

TABLE 2

| MORPHOLOGY OF HARD X-RAY SOURCES | |
|----------------------------------|------------|
| Morphology | Percentage |
| single | 30% |
| double | 41% |
| multiple/diffuse | 29% |

It is an imager based on Fourier synthesis with 64 elements, each one measuring the photon count rates, which are synthesised into an image by procedures based on the the maximum entropy method (Willingale 1981). The main capabilities of HXT are: (a) simultaneous imaging in 4 energy bands: *L* (13.9–22.7 keV), *M1* (22.7–32.7 keV), *M2* (32.7–52.7 keV), and *H* (52.7–92.8 keV); (b) field of view covering the whole sun; (c) angular resolution of 5 arcsec; (d) temporal resolution of 0.5 s; (e) total aperture of 60 cm² (Kosugi et al. 1992).

The Hard X-Ray Spectrometer (HXS) (Yoshimori et al. 1991) is a NaI scintillation counter and detects X-rays in the energy range 25–826 keV, in 32 channels, with a time resolution of 1 s, and also, in 2 channels, in high resolution mode, with time resolution of 0.125 s.

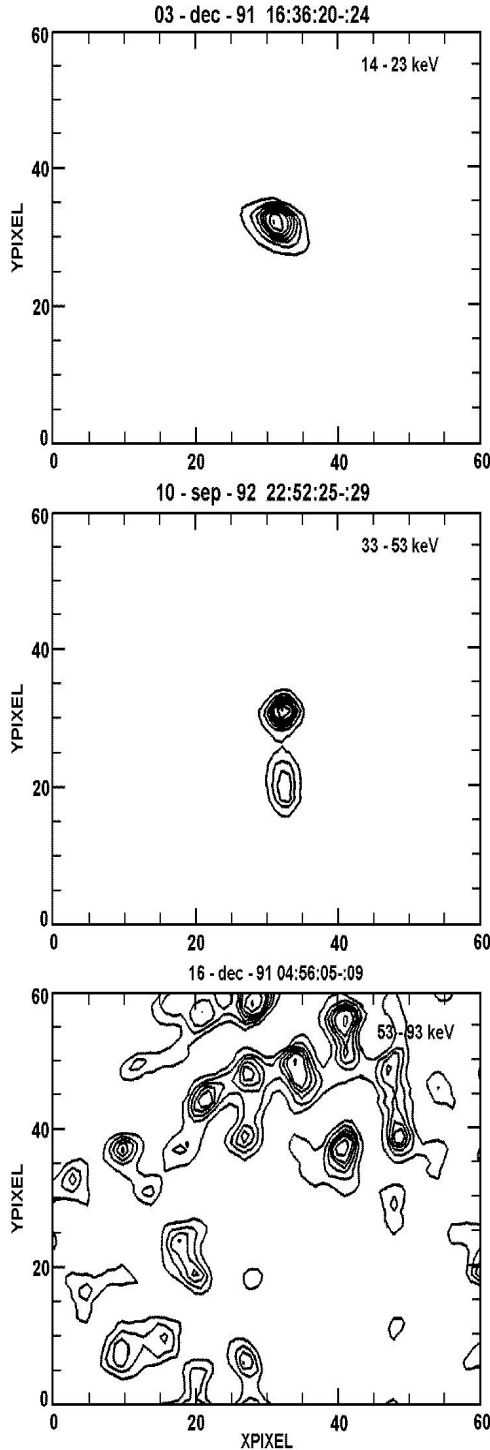


Fig. 2. Examples of contour maps obtained from HXT X-ray images for the peak time of the bursts, with integration time of 4 s, showing the different source morphologies: (top) single source (1991/Dec/03 16:36:20–24; 14–23 keV); (middle) double source (1991/Sep/10 22:52:25–29; 33–53 keV); (bottom) multiple source (1991Dec/16 04:56:05–09; 53–93 keV).

In order to carry out a study of the morphology and spectral behavior of hard X-ray sources, we have selected 17 solar flares observed simultaneously by the HXT and HXS instruments, between October 1991 and October 1993, corresponding to a total of 61 individual X-ray bursts (Table 1). Figure 1 shows an example of HXT hard X-ray time profiles. The bursts were selected according to the following criteria:

- (a) impulsive bursts consisting of multiple peaks;
- (b) individual peaks of duration < 30 s (typical “elementary flare burst” time scale; van Beek, Feiter, & de Jager 1976);
- (c) peak count rates in the $M2$ band of $\geq 3\sigma$ (σ is the standard deviation of the background level).

3. DATA ANALYSIS

3.1. Morphology of Hard X-Ray Sources

Synthesized images of the hard X-ray sources associated with the 17 selected flares were made in order to obtain information about the distribution and dimensions of the sources, and to complement information about the spectral behavior.

First, the source locations on the solar disk were determined. Then, the coordinates of the center of the image (64×64 pixels) were obtained for the 4 energy bands of HXT for each individual peak, with an integration time of 4 s. The resolution of the image is $2.47''/\text{pixel}$, corresponding to a total dimension of 158×158 arcsec. Thus, the angular size of the hard X-ray sources is about 20 arcsec.

The hard X-ray sources at the time of their peak emission were classified according to their morphology as follows: (a) single source identified in all 4 energy bands; (b) double discrete and separated sources, or lightly connected—the typical separation between double sources is about 30–40 arcsec; (c) multiple source structure, especially for the higher energy bands, or diffuse structure without a characteristic discrete source. Figure 2 shows images of X-ray sources presenting these three different morphologies. Table 2 gives the distribution of the sources.

3.2. Spectral Analysis

The spectral behavior of the hard X-ray emission is related to the population of emitting electrons and can thus provide information about electron distribution and acceleration processes during the flares.

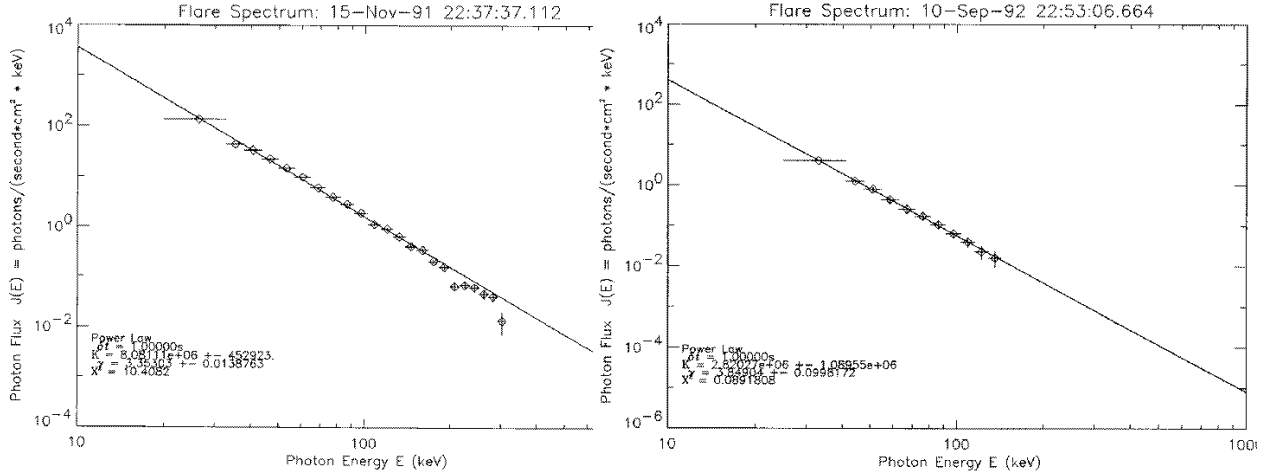


Fig. 3. Examples of fitted power-law spectra for the hard X-ray emission for peak time of bursts observed in: (top) 1991 November 15 (22:37:37.112 UT) and (bottom) 1992 September 10 (22:53:06.664 UT).

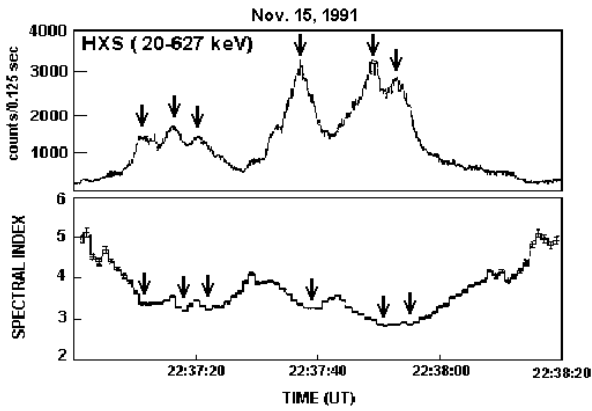


Fig. 4. Top: time profile of hard X-ray flare observed in 1991 November 15. Bottom: time evolution of the spectral index. Each individual peak shows a spectral index evolution as “soft-hard-soft”.

For the thick target model (Brown 1971), assuming a power-law distribution of injected electrons, the resultant hard X-ray spectrum observed is also a power-law of the form: $I(\epsilon) = a\epsilon^{-\gamma}$, where a is a factor of the Beta function and γ is the hard X-ray spectral index, which is related to the electron energy distribution spectral index, δ , as $\gamma = \delta - 1$ (Lin & Hudson 1976; Hudson, Canfield, & Kane 1978).

Thus, we have fitted a power-law spectrum to the hard X-ray emission, with integration time of 1 s, using the fitting routine HXS-FSP developed by McTiernan (Yohkoh Analysis Guide 1994) based on the thick target model. Figure 3 shows examples of the fitted power-law spectrum. For each event, we also obtained the time evolution of the spectral index for the whole time interval of the burst.

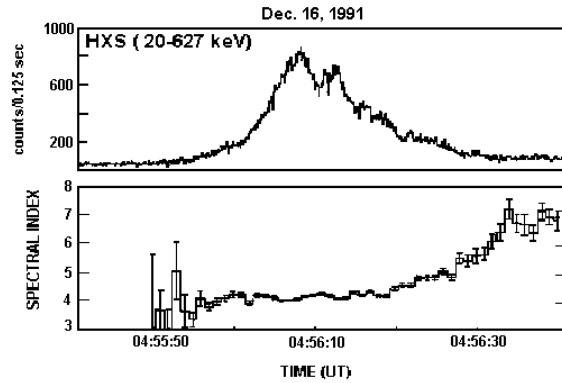


Fig. 5. Top: time profile of hard X-ray flare observed in 1991 December 16. Bottom: time evolution of the spectral index. The global behavior of the spectral index shows an evolution as “hard-hard-soft”.

The analysis of the time evolution of the spectral index showed that for $\sim 88\%$ of the individual bursts the behavior is typically “soft-hard-soft”, respectively, for rise, peak and decay phases (Figure 4). For only 2 cases ($\sim 12\%$) this tendency is not evident. For flares 7 and 9 in Table 1, the spectrum appears harder at rise and peak phases (approximately flat) and soft in the decay phase, i.e., “hard-hard-soft” (Figure 5). A histogram of the spectral index values at the peak time for the 61 individual bursts is given in Figure 6.

4. SUMMARY AND DISCUSSIONS

We have analyzed the morphology and spectral behavior of hard X-ray sources associated with 17 solar flares observed by the *Yohkoh* satellite. The

TABLE 3
SOURCES MORPHOLOGY AND PEAK-TIME SPECTRAL INDEX OF
THE 61 HARD X-RAY BURSTS

| Flare No. | Number of peaks | Morphology | Peak-time Spectral Index of each individual burst |
|-----------|-----------------|------------------|---|
| 1 | 2 | single | 4.7 / 6.4 |
| 2 | 1 | double | 3.7 |
| 3 | 4 | double | 2.9 / 3.0 / 3.6 / 3.6 |
| 4 | 4 | single | 2.9 / 3.0 / 3.3 / 3.4 |
| 5 | 3 | single | 3.7 / 3.8 / 3.8 |
| 6 | 4 | single | 2.8 / 2.8 / 3.2 / 3.3 |
| 7 | 1 | multiple | 4.1 |
| 8 | 4 | diffuse/complex | 3.5 / 4.1 / 4.1 / 4.2 |
| 9 | 5 | double | 3.9 / 4.0 / 4.2 / 4.5 / 4.6 |
| 10 | 4 | double connected | 3.8 / 3.8 / 4.0 / 4.1 |
| 11 | 8 | double connected | 5.1 / 5.2 / 5.3 / 5.4 / 5.5 / 5.6 / 5.8 / 5.8 |
| 12 | 3 | double connected | 4.6 / 5.6 / 6.4 |
| 13 | 1 | diffuse/complex | 4.9 |
| 14 | 5 | double | 2.9 / 3.3 / 3.4 / 3.8 / 3.9 |
| 15 | 6 | single | 3.0 / 3.2 / 3.3 / 3.5 / 4.2 / 4.3 |
| 16 | 3 | multiple | 3.5 / 3.9 / 4.2 |
| 17 | 3 | diffuse/complex | 2.6 / 2.7 / 2.9 |

image analysis has shown that the morphology of the sources is of three types: single sources (30%), double sources (41%), or multiple/complex, not clearly defined sources (29%), mainly at higher energy channels. Similar results were obtained by Sakao (1994).

The single sources may represent an impulsive source at the loop top, as Masuda (1994) has identified for flares in limb analysis, and are associated

with primary energy release of the flares, resulting from the magnetic reconnection process that occurs at the top of closed magnetic loops and that may cause the heating of plasma to temperatures up to 2×10^7 K, and the acceleration of particles in regions located at heights of the order of $1.2\text{--}4.5 \times 10^9$ cm above the photosphere (Fernandes et al. 2000).

The double sources, generally more common for impulsive hard X-ray emission (especially for energies ≥ 30 keV), are generated by a non-thermal Bremsstrahlung process, and are a signature of the energetic electrons accelerated during the flares which precipitated along the magnetic loops towards the footpoints.

Spectral analysis has shown that the time evolution of the spectral index for the majority of the bursts (88%) presents a typical “soft-hard-soft” behavior, for the initial, peak, and decay phases, respectively, characterizing an impulsive particle injection. For only 2 bursts is this behavior is evident: they show an almost flat spectrum for the initial and peak phases and a softer one for the decay phase, which suggests a gradual acceleration of the emitting electrons.

The results suggest that there is no evident correlation between the morphology of hard X-ray (dou-

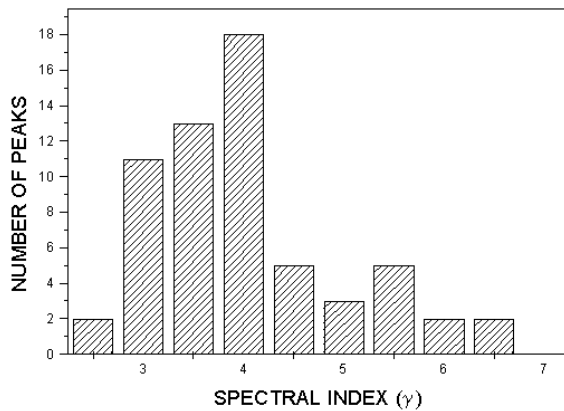


Fig. 6. Histogram of spectral index values for peak time of the 61 individual bursts.

ble or single) sources and the spectral behavior of emission during the event, hence that both double and single sources present spectral evolution typically “soft-hard-soft”, and only 2 events (1 double and 1 single) present “hard-hard-soft” spectrum evolution. Details of these studies are given by Fernandes (1997). The results obtained from the morphological and spectral analyses are summarized in Table 3.

The authors are grateful to the *Yohkoh* Team for providing the X-ray data and to S. R. Kane and J. M. McTiernan from Space Science Laboratory (UCB/USA) for data analysis support. This work was supported by CNPq (381647/97-8) and FAPESP (99/10529-0) scholarships. Thanks are due to the referee for helpful suggestions and comments.

REFERENCES

- Acton, L. W., et al. 1980, *Solar Phys.*, 65, 53
 Brown, J. C. 1971, *Solar Phys.*, 18, 489
 Duijveman, A., Hoyng, P., & Machado, M. E. 1982, *Solar Phys.*, 81, 137
 Fernandes, F. C. R. 1997, Ph.D. thesis, INPE (6396-TDI/612), São José dos Campos, Brazil
 Fernandes, F. C. R., Sawant, H. S., Meléndez, J. L., Benz, A. O., & Kane, S. R. 2000, *Adv. Space Res.*, 25, 1813
 Hoyng, P., Machado, M. E., & Duijveman, A. 1981, *ApJ*, 244, L153
 Hudson, H. S., Canfield, R. C., & Kane, S. R. 1978, *Solar Phys.*, 60, 137
 Kondo, I. 1982, *Proc. Hinotori Symp. on Solar Flares*, (Tokyo: Institute of Space and Astronautical Science), 3
 Kosugi, T., et al. 1991, *Solar Phys.*, 136, 17
 Kosugi, T., et al. 1992, *Pub. Astr. Soc. Japan*, 44, L45
 Lin, R. P., & Hudson, H. S. 1976, *Solar Phys.*, 50, 153
 Masuda, S. 1994, Ph.D. thesis, Univ. of Tokyo, Japan
 Masuda, S., Kosugi, T., Harra, H., Sakao, T., Shibata, K., & Tsuneta, S. 1995, *Pub. Astr. Soc. Japan*, 47, 677
 Ogawara, Y., et al. 1991, *Solar Phys.*, 136, 1
 Sakao, T. 1994 Ph.D. thesis, NAO, Tokyo, Japan
 Sakao, T., Kosugi, T., Masuda, S., Yaji, K., Koide, M. I., & Makishima, K. 1996, *Adv. Space Res.*, 17, 67
 Takakura, T., Tsuneta, S., Ohki, K., et al. 1983, *ApJ*, 270, L83
 van Beek, H. F., Feiter, L. D., & de Jager, C. 1976, *Space Res.*, 16, 819
 Yoshimori, M., Okudaira, K., Hirasima, Y., et al. 1991, *Solar Phys.*, 136, 69
 Willingale, R. 1981, *MNRAS*, 194, 359